

A Computationally Efficient Approach for Stochastic Reachability Set Analysis

Amit Jain* and Damién Gueho †
Pennsylvania State University, State College, PA-16802

Puneet Singla ‡
Pennsylvania State University, State College, PA-16802, USA

The reachability set is defined as the collection of all states which can be traversed from arbitrary initial conditions due to the application of admissible control. Three different probabilistic approaches to compute the reachability sets for a class of discrete time nonlinear systems is discussed. The main idea of the probabilistic approach is to consider the bounded control variables as random variables and represent the reachability sets as the level sets of the state probability density function. In the first approach, the computation of the state density function due to variation in control input at each time is made tractable by computing the M-fold convolution of state density function at each time. To overcome the significant challenge of taking multi-dimension convolution of state density function, the second approach computes the probability density function using the Principle of Maximum Entropy (PME). The third approach utilizes the Conjugate Unscented Transform (CUT) method to curtail the combinatorial growth of samples. Finally, three numerical example problems are considered to show the efficacy and utility of the proposed ideas.

I. Nomenclature

\mathbf{x}_k	=	system state variable $\in \mathbb{R}^n$ at time instant t_k
\mathbf{u}_k	=	control input variable $\in \mathbb{R}^r$ at time instant t_k
\mathcal{U}	=	set of admissible controls $\subset \mathbb{R}^r$
$p_{\mathbf{x}_k}(\mathbf{x}_k)$	=	density function corresponding to \mathbf{x}_k
$p_{\mathbf{u}_k}(\mathbf{u}_k)$	=	density function corresponding to \mathbf{u}_k
$\varphi_{\mathbf{x}_k}(\mathbf{s})$	=	characteristic function corresponding to \mathbf{x}_k
$\mathcal{R}(\mathbf{x}_0, \mathcal{U}, t_M)$	=	Reachability set at time t_M corresponding to initial state \mathbf{x}_0 and control \mathcal{U}

II. Introduction

Nonlinearity in the representation of the maneuvering Unmanned Autonomous Systems (UAS), uncertainties associated with system parameters, states and external disturbances together with its embedded control input provide significant challenges to automating the decision support system. Whether the autonomous system is an Unmanned Aerial Vehicle (UAV) flying at high speeds through a cluttered environment in the presence of wind gusts, a legged robot traversing rough terrain, a driverless car transversing an unknown environment, or a micro-air vehicle with noisy on-board sensing, the inability to take into account control input, system states and other uncertainties cause degradation to the performance of the control system, owing to the off-nominal operation of the autonomous system. The successful deployment of autonomous systems depends on rigorous guarantees on performance and safety through formal verification and validation methods. Quantitative measures to assess the excursions of the autonomous system motion from the designed trajectory are rigorous and exact for the linear systems. Approximate measures to quantify these excursions in the real world are poor and can lead to significant compromises in the overall performance. For

*Graduate Student, Department of Aerospace Engineering, Pennsylvania State University, State College, PA-16802, Email: axj307@psu.edu.

†Graduate Student, Department of Aerospace Engineering, Pennsylvania State University, State College, PA-16802, Email: djg76@psu.edu.

‡Associate Professor, AIAA Associate Fellow, AAS Fellow, Department of Aerospace Engineering, Pennsylvania State University, State College, PA-16802, Email: psingla@psu.edu.

instance, to ensure collision-free paths, advanced driver-assistance systems need to be capable of anticipating all potential actions of the driver without overly conservative assumptions. This requires performing on-line reachability analysis, i.e., computation of states that these vehicles can reach within a given time interval. To make it worse, the system states are typically not fully observable, e.g., a UAV might not have precise knowledge about its position. Thus, conducting accurate reachability analysis by definition requires reasoning about all possible trajectories from every possible state. This renders reachability analysis computationally intractable in practice [1]. This computational challenge is further compounded by the generally large size and nonlinearity of the system in consideration, and the practical need to obtain verification results for real-time motion planning.

Though one can obtain exact solution for reachability sets for linear time invariant systems, numerical approximations are necessary to compute the reachability sets for nonlinear systems. For certain classes of continuous dynamics, exact computation of the set of reachable states was shown in [2]. For more general classes of systems, numerical approximations have been explored in [3–8]. Alternately, the reachability questions are computed as zero-level set of the value function of an appropriate optimal control problem [9]. The computation of value function generally require the solution of the Hamilton-Jacobi-Bellman (HJB) or Issacs (HJI) equation. Various numerical techniques such as sum-of-squares [10, 11], Zonotope based approaches and Level Set Methods [12] have been developed for reachable set computations [13–15]. Various toolboxes such as Ellipsoidal[16], CORA (COntinuous Reachability Analyzer)[17], Trex[18], and HyTech[19] are also developed for the reachability analysis. Refs. [20, 21] have developed feedback controllers to generate largest time-limited backward reachable set while using the notion of occupation measure. Furthermore, ellipsoidal [22], support vector machine [23] and reason of interest approximation [24] are considered for reachability sets computations. While promising, all of these methods face a similar challenge with regards to computational scalability with the dimension of the system.

In this work, an alternative approach is proposed to compute the reachability sets in a computationally attractive manner. The main idea is to represent reachable sets as the probability density function of state variable at a given time. For this purpose, the admissible control set is assumed to be represented by a probability density function for control input at each time. Exploiting the fact that the control input at a specific time is independent of system states at that time, the computation of state density function at a given time can be posed as the convolution of density function for control input vector at previous time with a function of state density function at previous time. Furthermore, the Fourier transform of density function can be used to convert the convolution of density function to product of corresponding characteristic functions. Moreover, finite order statistical moments are computed to represent the spectral content of the density function and principle of maximum entropy is invoked to compute the state density function with highest entropy and computed moments. Finally, the Conjugate Unscented Transformation algorithm is used to compute the desired order statistical moments, which will help in curtailing the computational complexity associated with the computation of state density function.

The structure of paper is as follows: first, a brief introduction to reachability set problem is presented followed by the description of developed methods. Finally, the numerical simulation results are presented to show the efficacy of the proposed ideas.

III. Problem Formulation

The reachability flight envelope or set can be defined as the collection of all states which can be transversed from arbitrary initial conditions due to the application of admissible control. Let us consider the problem of computation of reachability set for a generic nonlinear system in the following form:

$$\mathbf{x}_{k+1} = f(\mathbf{x}_k) + G(\mathbf{x}_k)h(\mathbf{u}_k) \quad (1)$$

where $\mathbf{x}_k \in \mathbb{R}^n$ is the system state variable. $\mathbf{u}_k \in \mathcal{U} \subset \mathbb{R}^r$ represents the control input variable at time instant t_k . \mathcal{U} is the set of admissible controls and is assumed to be described a density function $p_{\mathbf{u}_k}(\mathbf{u}_k)$. For example, a uniform density function can be used to represent the admissible control set, \mathcal{U} which is assumed to be a hypercube. Similarly, a Gaussian density function can be used to represent an ellipsoidal admissible control set, \mathcal{U} . Hence the reachability sets of a system having an arbitrary initial state, \mathbf{x}_0 is the set of all possible states at time t_N , given $\mathbf{u}_k \in \mathcal{U}$. Mathematically, it can be represented as shown in Eq. (2)

$$\mathcal{R}(\mathbf{x}_0, \mathcal{U}, t_M) = \{\forall \mathbf{x} \in \mathbb{R}^n | \mathbf{u}_k \in \mathcal{U}, \forall k \in [0, M] \text{ s.t. } \mathbf{x}(t_M) = \mathbf{x}\} \quad (2)$$

The computation of reachability sets presents significant computational challenges due to the sampling of control inputs with states at each time. As discussed in the last section, there are a vast number of methods in the literature for

the computation of reachability sets. A heuristic method to compute reachability set will involve Monte Carlo based sampling of control input space. The main idea of the MC approach is to apply each bounded control input to every state variables at any point of time. Since this approach requires sampling of control variables from an admissible set at each time, this increases the number of samples exponentially over the number of time steps. This is because, after the first time step, one has to take all possible combinations of samples for \mathbf{x}_k and \mathbf{u}_k . For instance, if N_s samples of control variable are assumed at each time from admissible set \mathcal{U} , then there will be a total of N_s^M samples after M time steps.

This exponential growth can be visualized as shown in Figure (1). Starting from a single initial state \mathbf{x}_0 and after applying p control inputs which varies from u_{min} to u_{max} then $\mathbf{x}(t_1)$ will contain p number of states. Similarly, applying again p control inputs to these $\mathbf{x}(t_1)$ states will then give p^2 number of states at time t_2 . On increasing the number of time steps, this method requires very high computational time. Due to this reason, convolution method is computationally intractable for most onboard implementations. Therefore, there aroused a need for exploring other methods which are efficient and can be implemented for onboard applications.

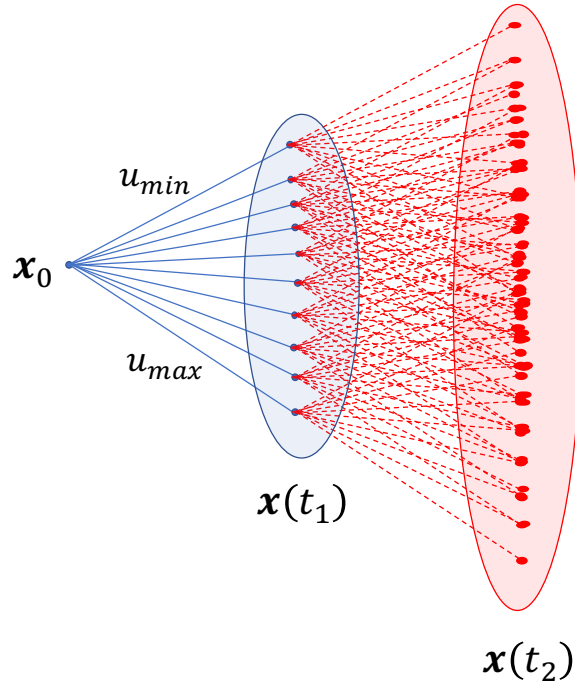


Fig. 1 Exponential Growth in Samples to Compute the Reachability Set.

A. Convolution Method

In this section, a new approach to compute the reachability set is presented, which avoids the combinatorial growth of samples. The central idea of this approach is to pose the computation of state density function at any time k , $p_{\mathbf{x}_k}(\mathbf{x}_k)$ as the convolution of two probability density functions to avoid the exponential growth in samples. In this method, the independence of the state variable \mathbf{x}_k and control input \mathbf{u}_k at time t_k is also exploited.

For this purpose, let us consider an affine control to the system at each time instance. Hence, the system response at time $k + 1$ (represented by \mathbf{x}_{k+1}) from Eq. (1) can be written as

$$\mathbf{x}_{k+1} = f(\mathbf{x}_k) + \mathbf{u}_k \quad (3)$$

Exploiting the fact that \mathbf{x}_k and \mathbf{u}_k are independent of each other and writing these as a function of two independent random vectors, \mathbf{v} and \mathbf{w} :

$$\mathbf{x}_{k+1} = \mathbf{v} + \mathbf{w} \quad (4)$$

where $\mathbf{v} = f(\mathbf{x}_k)$ and $\mathbf{w} = \mathbf{u}_k$. In general case, the probability density function for $\mathbf{x}(k+1)$ can be written as:

$$p_{\mathbf{x}_{k+1}}(\mathbf{x}_{k+1}) = \int p_{\mathbf{v},\mathbf{w}}(\mathbf{x}_{k+1} - \mathbf{w}, \mathbf{w}) d\mathbf{w} \quad (5)$$

If \mathbf{v} and \mathbf{w} are independent of each other, then the aforementioned equation for $p_{\mathbf{x}_{k+1}}(\mathbf{x}_{k+1})$ reduces to the following *convolution of density functions*[25]:

$$p_{\mathbf{x}_{k+1}}(\mathbf{x}_{k+1}) = \int p_{\mathbf{v}}(\mathbf{x}_{k+1} - \mathbf{w}) p_{\mathbf{w}}(\mathbf{w}) d\mathbf{w} \quad (6)$$

In other words, $p(\mathbf{x}_{k+1})$ can be computed as a convolution of derived density function for $\mathbf{v} = f_k = f(\mathbf{x}_k)$ and density function for $\mathbf{w} = \mathbf{u}_k$ as,

$$\begin{aligned} p_{\mathbf{x}_{k+1}}(\mathbf{x}_{k+1}) &= p_{f_k}(\mathbf{x}_{k+1} - \mathbf{u}_k) \star p_{\mathbf{u}_k}(\mathbf{u}_k) \\ &= \int p_{f_k}(\mathbf{x}_{k+1} - \mathbf{u}_k) p_{\mathbf{u}_k}(\mathbf{u}_k) d\mathbf{u}_k \\ &= \int p_{\mathbf{u}_k}(\mathbf{x}_{k+1} - f_k) p_{f_k}(f_k) d\mathbf{x}_k \end{aligned} \quad (7)$$

Also, it should be noted that p_{f_k} is sometimes known as *derived density function* since it can be derived from the density function of \mathbf{x}_k according to Eq. (8) [25]:

$$p_{f_k}(f_k) = p_{\mathbf{x}_k} \left(f_k^{-1}(\mathbf{x}_{k+1}) \right) \left\| \frac{\partial f_k^{-1}(\mathbf{x}_{k+1})}{\partial \mathbf{x}_{k+1}} \right\| \quad (8)$$

where $\left\| \frac{\partial f_k^{-1}(\mathbf{x}_{k+1})}{\partial \mathbf{x}_{k+1}} \right\|$ is the absolute value of the Jacobian determinant. Hence, to compute the density function $p_{\mathbf{x}_{k+1}}$, it is only required to sample the space of \mathbf{u}_k . The iterative application of this result can be used to compute the state density function $p(\mathbf{x}_N)$, and hence the reachability set $\mathcal{R}(\mathbf{x}_0, \mathcal{U}, t_M)$.

The probability density function for state and control variables can also be represented as histograms. For the computation of reachability set using histograms, reachability set $\mathcal{R}(\mathbf{x}_0, \mathcal{U}, t_M)$ corresponds to $N - 1$ convolutions of histograms for $f(\mathbf{x}_k)$ and \mathbf{u}_k . Thus, it is clear that the computation of reachability set through convolution of density functions reduces the dimensionality of the problem for stochastic analysis. However, the convolution of high-resolution histograms representing state and control density functions can be computationally demanding due to the challenges associated with the discretization and histogram generation in multi-dimension space. To overcome this significant challenge of evaluating the state density function, we exploited a fact that the characteristic function of a density function is its Fourier transform in multiple dimensions. The characteristic function is defined in Eq. (9) as,

$$\varphi_{\mathbf{x}_k}(\mathbf{s}) = \mathbb{E} \left[e^{i\mathbf{s}^T \mathbf{x}_k} \right] = \int e^{i\mathbf{s}^T \mathbf{x}_k} p_{\mathbf{x}_k}(\mathbf{x}_k) d\mathbf{x}_k \quad (9)$$

Now, by virtue of convolution theorem [26], the convolution of density functions in Eq. (7) can be written as the product of corresponding characteristic functions:

$$\varphi_{\mathbf{x}_{k+1}}(\mathbf{s}) = \varphi_{f_k}(\mathbf{s}) \varphi_{\mathbf{u}_k}(\mathbf{s}) \quad (10)$$

Hence rather than taking the convolution of density functions, the product of corresponding characteristic functions is taken. Although it can be challenging to compute the analytical expression for the characteristic function, the main advantage of the characteristic function is that one can obtain all the statistical moments of the random vector \mathbf{x}_{k+1} by differentiating it. The density function representation in terms of the finite number of statistical moments is equivalent to storing the first few Fourier coefficients of a periodic function. Also, it is more efficient to propagate the statistical moments than the computation of convolved density function. Therefore, focus was on computing the statistical moments of the convolved density function as a function of the moments of f_k and \mathbf{u}_k at each time instant. Since the statistical moments behaves like Fourier coefficients, one can obtain a better description of the state density function by computing higher order moments of \mathbf{x}_{k+1} . Furthermore, the state density function $p_{x_M}(x_M)$ and hence the reachability set, $\mathcal{R}(\mathbf{x}_0, \mathcal{U}, t_M)$ can then be obtained from propagated statistical moments by an application of the principle of maximum entropy (PME) as shown in the next section.

B. Principle of maximum entropy

In this section, the Principle of maximum entropy to overcome the significant challenges of evaluating the state density function is discussed. As the name suggests, PME finds the probability density function representing the highest uncertainty (entropy) with the same set of moments. This seems intuitive since any additional information in terms of moment constraints will lead to a density function that is better in the sense that it has less uncertainty. The PME can be mathematically framed according to Eq. (11) and Eq. (12) [27–29].

$$\max_{p_{\mathbf{x}_{k+1}}} : - \int p_{\mathbf{x}_{k+1}}(\mathbf{x}_{k+1}) \ln\{p_{\mathbf{x}_{k+1}}(\mathbf{x}_{k+1})\} d\mathbf{x}_{k+1} \quad (11)$$

$$s.t. : \int g_i(\mathbf{x}_{k+1}) p_{\mathbf{x}_{k+1}}(\mathbf{x}_{k+1}) d\mathbf{x}_{k+1} = M_i \quad i = 1, 2, \dots, N_m \quad (12)$$

where M_i are known finite scalar values. The set of functions $g_i(\mathbf{x}_{k+1})$ have to be independent to form a well-posed problem and are chosen to be multidimensional monomials that represent moments of various order. The aforementioned optimization problem is concave in nature and results in a member of the exponential family of density functions that represents the highest uncertainty with an identical set of moments [29, 30] given by Eq. (13).

$$p_{\mathbf{x}_{k+1}}(\mathbf{x}_{k+1}) = \exp\left\{\sum_{i=1}^{N_m} \lambda_i g_i(\mathbf{x}_{k+1})\right\} \quad (13)$$

where, λ_i are Lagrange multipliers and are found by solving the following system of N_m nonlinear equations:

$$\int g_i(\mathbf{x}_{k+1}) \exp\left\{\sum_{i=1}^{N_m} \lambda_i g_i(\mathbf{x}_{k+1})\right\} d\mathbf{x}_{k+1} = M_i \quad (14)$$

$$i = 1, 2, \dots, N_m$$

Efficient numerical equation solvers (such as in Ref. [29]) can be used to solve the system of nonlinear equations. When $g_i(\mathbf{x}_{k+1})$ are monomials, the exponential function can become insensitive to the Lagrange multipliers corresponding to the lower order monomials[31] since, the higher degree monomials grow faster. To avoid the sensitivity issue, the moments constraint equations have to be re-scaled to improve the rate of convergence[31]. The procedure outlined in Ref.[31] is used to solve the resulting system of equations through the application of Broyden-Fletcher-Goldfarb-Shanno (BFGS) algorithm [32]. It should be noticed that if g_i 's correspond to first and second central moments, then PME results in a Gaussian density function with mean and covariance described by M_i 's. This corresponds to the ellipsoidal approximation of the reachability set. One can obtain a more accurate description of the reachability set by including higher order moment constraints in the formulation of PME.

It can be seen that the computation of reachability sets through statistical moments is preferable as it is easier to compute moments accurately rather than computing multi-dimensional histograms. However, PME requires a good initial guess and sometimes results in slow convergence depending upon the nature of the optimization problem. In addition, MC runs are generally required to compute the desired order statistical moments which can be numerically expensive to evaluate accurately these integrals. Therefore, an alternate approach is presented in the next section where the recently developed Conjugate Unscented Transformation(CUT) scheme is used to compute the desired order moments. The independence of the state and the control input is exploited to compute the statistical moments in a lower dimensional space while the CUT method guarantees a fixed number of points at each time step.

C. Computation using Statistical Moments

This section will discuss the problem description, formulation and specific assumptions of our approach. To compute the desired order statistical moments efficiently, the fact that the state variable \mathbf{x}_k at time t_k is independent of control input variable \mathbf{u}_k at time t_k is again exploited.

Let us consider a general non-linear system given by Eq. (1) in an index notation as shown by Eq. (15).

$$x_{k+1}^\alpha = f^\alpha(\mathbf{x}_k) + G^{\alpha\beta}(\mathbf{x}_k) h^\beta(\mathbf{u}_k), \quad \alpha = 1, 2, \dots, n, \quad \beta = 1, 2, \dots, r \quad (15)$$

where x_{k+1}^α and $f^\alpha(\mathbf{x})$ represent the α^{th} component of vectors \mathbf{x}_{k+1} and $f(\mathbf{x}_k)$, respectively. Similarly, $G^{\alpha\beta}(\mathbf{x}_k)$ represents the $\alpha\beta$ component of the matrix $G(\mathbf{x}_k)$. Notice that in index notation the repetition of the index corresponds

to summation and hence can be written as,

$$G^{\alpha\beta}(\mathbf{x}_k) h^\beta(\mathbf{u}_k) \equiv \sum_{\beta=1}^r G^{\alpha\beta}(\mathbf{x}_k) h^\beta(\mathbf{u}_k) \quad (16)$$

Now, the expected value of \mathbf{x}_{k+1}^α can be formulated as:

$$\mathbb{E}[x_{k+1}^\alpha] = \mathbb{E}[f^\alpha(\mathbf{x}_k)] + \mathbb{E}[G^{\alpha\beta}(\mathbf{x}_k) h^\beta(\mathbf{u}_k)] \quad (17)$$

Making use of the fact that \mathbf{x}_k is an independent random vector from \mathbf{u}_k , the second term in the aforementioned equation can be put together as:

$$\mathbb{E}[G^{\alpha\beta}(\mathbf{x}_k) h^\beta(\mathbf{u}_k)] = \mathbb{E}[G^{\alpha\beta}(\mathbf{x}_k)] \mathbb{E}[h^\beta(\mathbf{u}_k)] \quad (18)$$

Hence, the first order moment for state vector x_{k+1} can be written as:

$$\mathbb{E}[x_{k+1}^\alpha] = \mathbb{E}[f^\alpha(\mathbf{x}_k)] + \mathbb{E}[G^{\alpha\beta}(\mathbf{x}_k)] \mathbb{E}[h^\beta(\mathbf{u}_k)] \quad (19)$$

Since the density function for \mathbf{x}_k and \mathbf{u}_k is known and hence the first order moment for \mathbf{x}_{k+1} can be computed by separately sampling \mathbf{x}_k and \mathbf{u}_k space. Similarly, the second order moments can be computed as follows,

$$\mathbb{E}[x_{k+1}^\alpha x_{k+1}^\beta] = \mathbb{E}[(f^\alpha(\mathbf{x}_k) + G^{\alpha a}(\mathbf{x}_k) h^a(\mathbf{u}_k)) (f^\beta(\mathbf{x}_k) + G^{\beta b}(\mathbf{x}_k) h^b(\mathbf{u}_k))] \quad (20)$$

$$\begin{aligned} &= \mathbb{E}[f^\alpha(\mathbf{x}_k) f^\beta(\mathbf{x}_k)] + \mathbb{E}[f^\alpha(\mathbf{x}_k) G^{\beta b}(\mathbf{x}_k) h^b(\mathbf{u}_k)] \\ &+ \mathbb{E}[f^\beta(\mathbf{x}_k) G^{\alpha a}(\mathbf{x}_k) h^a(\mathbf{u}_k)] + \mathbb{E}[G^{\alpha a}(\mathbf{x}_k) h^a(\mathbf{u}_k) G^{\beta b}(\mathbf{x}_k) h^b(\mathbf{u}_k)], \end{aligned} \quad (21)$$

$\alpha, \beta = 1, 2, \dots, n, \quad a, b = 1, 2, \dots, r$

Once again, making use of the fact that \mathbf{x}_k is independent of \mathbf{u}_k , the aforementioned expression can be simplified as given by Eq. (22)

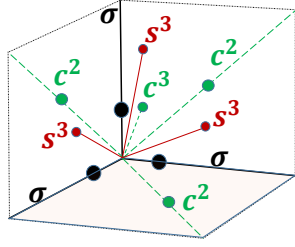
$$\begin{aligned} \mathbb{E}[x_{k+1}^\alpha x_{k+1}^\beta] &= \mathbb{E}[f^\alpha(\mathbf{x}_k) f^\beta(\mathbf{x}_k)] + \mathbb{E}[f^\alpha(\mathbf{x}_k) G^{\beta b}(\mathbf{x}_k)] \mathbb{E}[h^b(\mathbf{u}_k)] \\ &+ \mathbb{E}[f^\beta(\mathbf{x}_k) G^{\alpha a}(\mathbf{x}_k)] \mathbb{E}[h^a(\mathbf{u}_k)] + \mathbb{E}[G^{\alpha a}(\mathbf{x}_k) G^{\beta b}(\mathbf{x}_k)] \mathbb{E}[h^a(\mathbf{u}_k) h^b(\mathbf{u}_k)] \end{aligned} \quad (22)$$

Likewise, the third order moment can also be computed and simplified using the steps mentioned earlier and is finally given by Eq. (24).

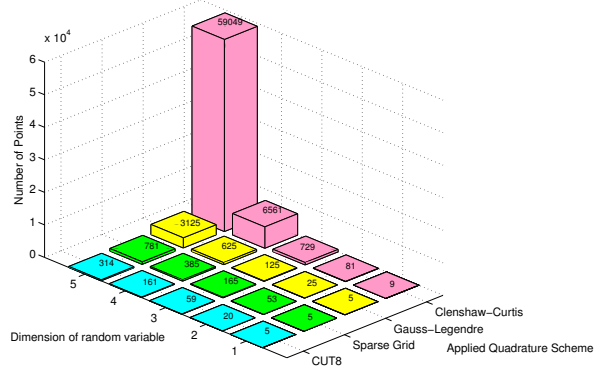
$$\begin{aligned} \mathbb{E}[x_{k+1}^\alpha x_{k+1}^\beta x_{k+1}^\gamma] &= \mathbb{E}[(f^\alpha(\mathbf{x}_k) + G^{\alpha a}(\mathbf{x}_k) h^a(\mathbf{u}_k))^3] \\ &= \mathbb{E}[f^\alpha(\mathbf{x}_k) f^\beta(\mathbf{x}_k) f^\gamma(\mathbf{x}_k)] + \mathbb{E}[f^\alpha(\mathbf{x}_k) f^\beta(\mathbf{x}_k) G^{\gamma c}(\mathbf{x}_k) h^c(\mathbf{u}_k)] \\ &+ \mathbb{E}[f^\alpha(\mathbf{x}_k) G^{\beta b}(\mathbf{x}_k) h^b(\mathbf{u}_k) f^\gamma(\mathbf{x}_k)] + \mathbb{E}[f^\alpha(\mathbf{x}_k) G^{\beta b}(\mathbf{x}_k) h^b(\mathbf{u}_k) G^{\gamma c}(\mathbf{x}_k) h^c(\mathbf{u}_k)] \\ &+ \mathbb{E}[G^{\alpha a}(\mathbf{x}_k) h^a(\mathbf{u}_k) f^\beta(\mathbf{x}_k) f^\gamma(\mathbf{x}_k)] + \mathbb{E}[G^{\alpha a}(\mathbf{x}_k) h^a(\mathbf{u}_k) f^\beta(\mathbf{x}_k) G^{\gamma c}(\mathbf{x}_k) h^c(\mathbf{u}_k)] \\ &+ \mathbb{E}[G^{\alpha a}(\mathbf{x}_k) h^a(\mathbf{u}_k) G^{\beta b}(\mathbf{x}_k) h^b(\mathbf{u}_k) f^\gamma(\mathbf{x}_k)] \\ &+ \mathbb{E}[G^{\alpha a}(\mathbf{x}_k) h^a(\mathbf{u}_k) G^{\beta b}(\mathbf{x}_k) h^b(\mathbf{u}_k) G^{\gamma c}(\mathbf{x}_k) h^c(\mathbf{u}_k)] \end{aligned} \quad (23)$$

$\alpha, \beta, \gamma = 1, 2, \dots, n, \quad a, b, c = 1, 2, \dots, r$

$$\begin{aligned} \mathbb{E}[x_{k+1}^\alpha x_{k+1}^\beta x_{k+1}^\gamma] &= \mathbb{E}[f^\alpha(\mathbf{x}_k) f^\beta(\mathbf{x}_k) f^\gamma(\mathbf{x}_k)] + \mathbb{E}[f^\alpha(\mathbf{x}_k) f^\beta(\mathbf{x}_k) G^{\gamma c}(\mathbf{x}_k)] \mathbb{E}[h^c(\mathbf{u}_k)] \\ &+ \mathbb{E}[f^\alpha(\mathbf{x}_k) G^{\beta b}(\mathbf{x}_k) f^\gamma(\mathbf{x}_k)] \mathbb{E}[h^b(\mathbf{u}_k)] \\ &+ \mathbb{E}[f^\alpha(\mathbf{x}_k) G^{\beta b}(\mathbf{x}_k) G^{\gamma c}(\mathbf{x}_k)] \mathbb{E}[h^b(\mathbf{u}_k) h^c(\mathbf{u}_k)] \\ &+ \mathbb{E}[G^{\alpha a}(\mathbf{x}_k) f^\beta(\mathbf{x}_k) f^\gamma(\mathbf{x}_k)] \mathbb{E}[h^a(\mathbf{u}_k)] \\ &+ \mathbb{E}[G^{\alpha a}(\mathbf{x}_k) f^\beta(\mathbf{x}_k) G^{\gamma c}(\mathbf{x}_k)] \mathbb{E}[h^a(\mathbf{u}_k) h^c(\mathbf{u}_k)] \\ &+ \mathbb{E}[G^{\alpha a}(\mathbf{x}_k) G^{\beta b}(\mathbf{x}_k) f^\gamma(\mathbf{x}_k)] \mathbb{E}[h^a(\mathbf{u}_k) h^b(\mathbf{u}_k)] \\ &+ \mathbb{E}[G^{\alpha a}(\mathbf{x}_k) G^{\beta b}(\mathbf{x}_k) G^{\gamma c}(\mathbf{x}_k)] \mathbb{E}[h^a(\mathbf{u}_k) h^b(\mathbf{u}_k) h^c(\mathbf{u}_k)] \end{aligned} \quad (24)$$



(a) Schematic of CUT Cubature Points in 3-D.



(b) Comparison of number of 8^{th} order quadrature points

Fig. 2 The Schematic of CUT points and growth of CUT points with number of random variables.

Similarly, one can obtain the expressions for computing any desired order statistical moments. However, in this paper, statistical moments up to the 2^{nd} order is used to calculate the reachability set. Notice here that the 1^{st} order statistical moment corresponds to the mean, the 2^{nd} order statistical moment corresponds to the variance, 3^{rd} order statistical moment corresponds to the Skewness(measure of asymmetry) and 4^{th} order statistical moment corresponds to Kurtosis(measure of the tailedness). Now to compute the desired order moments for each module, one needs to sample the \mathbf{x}_k and \mathbf{u}_k spaces. The Monte Carlo (MC) methods traditionally used to evaluate statistical moments suffer from slow convergence rates. An efficient alternative to random sampling is the quadrature scheme, such as the Gaussian Quadrature that uses deterministic M^m sample points in m dimensions, chosen to reproduce $2M - 1$ moments of the density function. For example, the number of points required to evaluate the expectation integral with only 5 points along each direction in a 6-dimensional space is $5^6 = 15,625$. Fortunately, the Gaussian quadrature rule is not minimal for $m \geq 2$ [33], and there exist quadrature rules requiring fewer points in high dimensions [34]. For example, the Unscented Transformation (UT) is exact to degree 2 but with linear growth of points with dimension. However, UT cannot be used to reproduce higher order moments.

A non-product quadrature rule known as the *Conjugate Unscented Transformation* (CUT) [35, 36] has been employed. The CUT approach can be considered an extension of the conventional UT method that satisfies additional higher order moment constraints. Rather than using tensor products as in Gauss quadrature, the CUT approach judiciously selects special structures to extract symmetric quadrature points constrained to lie on specially defined axes as shown in Figure (2(a)). These new sets of so-called sigma points are guaranteed to exactly evaluate expectation integrals involving polynomial functions with significantly fewer points. Figure (2(b)) represents the number of quadrature points required, for 8^{th} order accuracy, by different quadrature schemes (CUT, Gauss-Legendre, Clenshaw-Curtis, and Sparse Grid), for a uniform random variable, as a function of the dimensionality of the random variable. More details about the CUT methodology and its comparison with conventional quadrature rules can be found in Ref. [35–43].

In this work, the computation of the statistical moments were limited up to 2^{nd} order. The following lists the required

CUT approximation of various expected values:

$$\mathbb{E}[f^\alpha(\mathbf{x}_k)] = \sum_{i=1}^N w_x^i f^\alpha(\mathbf{x}_k^i), \quad \mathbb{E}[G^{\alpha\beta}(\mathbf{x}_k)] = \sum_{i=1}^N w_x^i G^{\alpha\beta}(\mathbf{x}_k^i) \quad (25)$$

$$\mathbb{E}[f^\alpha(\mathbf{x}_k) f^\beta(\mathbf{x}_k)] = \sum_{i=1}^N w_x^i f^\alpha(\mathbf{x}_k^i) f^\beta(\mathbf{x}_k^i) \quad (26)$$

$$\mathbb{E}[f^\alpha(\mathbf{x}_k) G^{\beta b}(\mathbf{x}_k)] = \sum_{i=1}^N w_x^i f^\alpha(\mathbf{x}_k^i) G^{\beta b}(\mathbf{x}_k^i) \quad (27)$$

$$\mathbb{E}[h^b(\mathbf{u}_k)] = \sum_{i=1}^N w_u^i h^b(\mathbf{u}_k^i) \quad (28)$$

$$\mathbb{E}[G^{\alpha a}(\mathbf{x}_k) G^{\beta b}(\mathbf{x}_k)] = \sum_{i=1}^N w_x^i G^{\alpha a}(\mathbf{x}_k^i) G^{\beta b}(\mathbf{x}_k^i) \quad (29)$$

$$\mathbb{E}[h^a(\mathbf{u}_k) h^b(\mathbf{u}_k)] = \sum_{i=1}^N w_u^i h^a(\mathbf{u}_k^i) h^b(\mathbf{u}_k^i) \quad (30)$$

where w_x^i and w_u^i corresponds to CUT points weight for density functions $p_{\mathbf{x}_k}(\mathbf{x}_k)$ and $p_{\mathbf{u}_k}(\mathbf{u}_k)$, respectively.

One can also compute expectation integrals appearing in the expressions for higher order moments through the application of the CUT approach. After computing desired order statistical moments at each time, one can construct the state density function through the application of various density approximation tools such as PME or SOS. However, one needs to generate samples from newly approximated density function to compute statistical moments at the next time step. Since CUT quadrature points are given for only Gaussian and uniform density functions, one can expand the state variable at each time in terms of polynomial series of standardized Gaussian or uniform variable, ξ

$$x_k^\alpha = \sum_{i=0}^N x_{k_i}^\alpha \phi_i(\xi) \Rightarrow \mathbf{x}_k = \mathbf{X}_{pc}(t)\Phi(\xi), \quad \alpha = 1, 2, \dots, n \quad (31)$$

where, $\phi_k(\xi)$ are orthogonal polynomials associated with the assumed probability distribution for the input variables ξ (Hermite polynomials for normally distributed parameters, Legendre polynomials for uniform distribution, etc.) and can be computed through the application of the Gram-Schmidt orthogonalization process. Here \mathbf{X} are matrices composed of coefficients of the polynomial expansion for \mathbf{x} . Now, the known statistical moments of \mathbf{x} at a specific time step, k , can be written in terms of the unknown polynomial coefficients:

$$\mathbb{E}[x_k^\alpha] = x_{k_0}^\alpha, \quad \alpha = 1, 2, \dots, n \quad (32)$$

$$\mathbb{E}[x_k^\alpha x_k^\beta] = \sum_{i=1}^N x_{k_i}^\alpha x_{k_i}^\beta \mathbb{E}[\phi_i(\xi)\phi_i(\xi)], \quad \alpha, \beta = 1, 2, \dots, n \quad (33)$$

Note that the expected values of the product of the gPC basis functions, $\mathbb{E}[\phi_k(\xi)\phi_k(\xi)]$, are known from the properties of the functions. Depending on the order of the polynomial expansion, the desired moment constraints and the dimension of \mathbf{x} , the resulting equations can be over-determined, properly determined, or under-determined. In Ref. [44], an approach is presented to compute these unknown polynomial series coefficients from desired order moment constraint equations. Now, one can generate an estimate of the state density function of \mathbf{x} by substituting random samples of ξ in Eq. (31). Of course, there will be an improvement in accuracy when one goes to higher order PC coefficients and compute higher order moments. However, there is always a trade-off between the accuracy and the computational cost. Finally, the main steps of the proposed approach can be enumerated as follows:

- Step 1: Generate CUT samples from standard Gaussian or Uniform random variables.
- Step 2: Compute CUT samples for state variables through the application of Eq. (31). If the state density function is assumed to be Gaussian or uniform, then only two of the coefficients will be non-zero.
- Step 3: Compute multi-dimensional expectation integrals while using Eq. (25)-Eq. (30) to compute desired order statistical moments for state variable of Eq. (19)-Eq. (22).
- Step 4: Recompute polynomial series coefficients through moment matching and go to Step 2.

IV. Numerical Results

To show the efficacy of the proposed approaches in approximating the reachability set, three numerical examples are considered. First the reachability set of N-pendulum systems is presented, followed by an airplane flying in wind gusts is exhibited, and finally reachability set of Dubin's car Model is shown.

A. Pendulum Problem

In this section, the reachability set of N-pendulums which are connected from one end to another were computed. The reachability set for a 2-pendulum system is depicted in Fig. 3, where L_1, L_2 is the length, θ_1, θ_2 is the angle and (x_1, y_1) and (x_2, y_2) is the position of the 1st and 2nd pendulum respectively. A comparison of MC and convolution approach is also shown. The Monte Carlo approach here involves every possible combination of the first pendulum and applies the feasible control input to it for computing the reachability set of the second pendulum. However, in convolution approach, the reachability set is computed by convolving the probability density function of each pendulum.

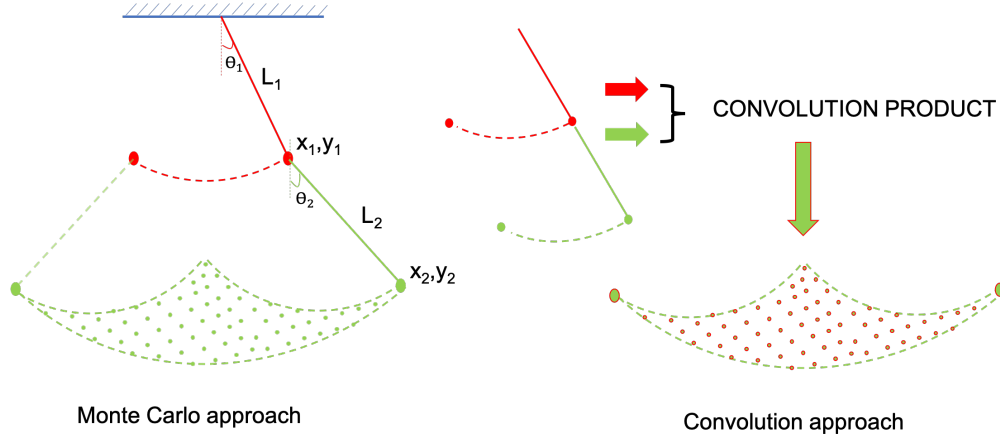


Fig. 3 Monte Carlo and Convolution methods Illustration on a 2 - pendulum system

The dynamics of the N connected pendulums can be written as:

$$x_N = \sum_{i=1}^N L_i \sin(\theta_i), \quad y_N = \sum_{i=1}^N L_i \cos(\theta_i)$$

where x_N, y_N is the position of the N^{th} pendulum.

To compute the reachability set of the N^{th} pendulum, the control input θ_i is bounded uniformly between -60° to 60° . First, the computation of reachability set with the MC method by taking 100,000 MC points for each pendulum is performed. After that, the contrast between the convolution and the PME method is made using the same number of MC points.

The comparison of reachability set for 3, 5, 7, and 9-pendulums can be seen in Fig. 4 based on the methods described above. Notice that the reachability set always come out to be symmetric along the y-axis and increases in a non symmetric manner along the x-axis with every increase in the number of pendulums. As seen in the first column of Fig. 4, the probability contours which are computed both with convolution and Monte Carlo method (shown in cyan color) are shown. For the 3-pendulum system, it can be noticed that the convolution contours match the shape of the MC points precisely. For the 5, 7, and 9-pendulums, the contours are also able to capture the reachability set in a reasonably good manner. For the PME method, the second, third and fourth column of Fig. 4 represents the 2nd, 3rd and 4th order PME results. As expected, the 2nd order PME contours are coming out to be ellipsoidal corresponding to the Gaussian assumption. As the order of the moment constraints is increased in PME, the PME solution is able to capture non-Gaussian shapes. For comparison between the PME and convolution method, it can be seen that the convolution can capture the MC points pretty accurately, but the 4th order PME results fail to do so. For instance, the 4th order PME results for the 3-pendulum system fails to capture the outline shape, but the convolution can capture it accurately.

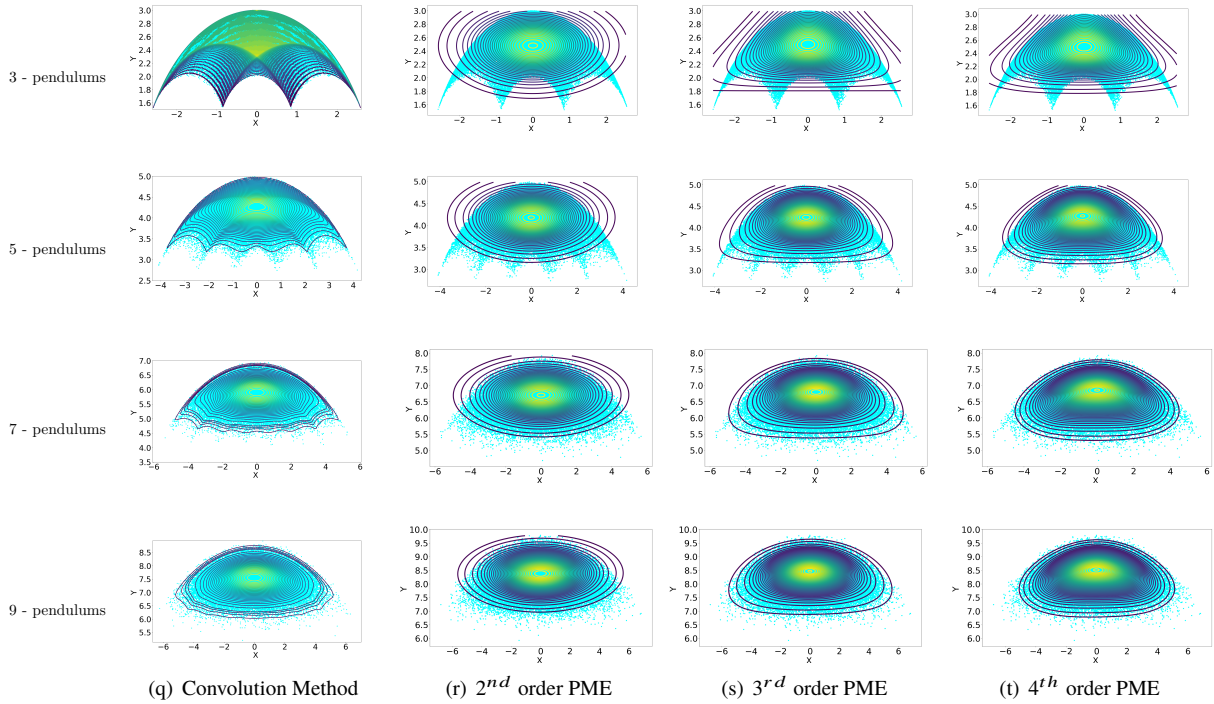


Fig. 4 Comparison of Various Approaches in Approximating Reachability Set of N-Pendulums

B. 2D Airplane Problem

In this section, the reachability set of an airplane flying in two dimensions is calculated based on Ref. [46]. In this example, the external disturbances are also accounted. These disturbances can arise due to the wind gusts alongside the noise in the control inputs. The full non-linear dynamics of the system are given by:

$$\begin{aligned}\dot{x} &= -v \cos \psi + \omega \\ \dot{y} &= v \sin \psi\end{aligned}\quad (34)$$

where x and y represents the position of vehicle in x and y direction respectively and ψ is the yaw angle. The control input v represents the forward speed of the plane, and w represents the cross-wind. Note that this is also a type of Dubin's model, which is considered in the next section.

This continuous-time Airplane model can be discretized by approximating time derivatives with a finite difference as,

$$\begin{aligned}x_{k+1} &= x_k + (-v \cos \psi(t) + w(t))\Delta t \\ y_{k+1} &= y_k + v \sin \psi(t)\Delta t\end{aligned}\quad (35)$$

By choosing an appropriate time step Δt , the reachability set can be computed at any time instance. For calculating the numerical results, the zero initial conditions, i.e., $x_0 = 0$ and $y_0 = 0$ are assumed. The speed of the airplane, cross-wind, and the yaw angle is varied between the following bounds for computing the reachability set:

$$\begin{aligned}9.5m/s &\leq v \leq 10.5m/s \\ -0.3m/s &\leq w \leq 0.3m/s \\ -10deg &\leq \psi \leq 10deg\end{aligned}\quad (36)$$

The reachability set of the airplane is computed with the aforementioned approaches by using the discrete-time model given in Eq. (35) and by applying the bounds as given in Eq. (36). The ground truth is generated by taking

100,000 MC samples at each time step, and Δt is chosen to be 0.5s. This heuristic approach will serve as the ground truth for the comparison with the proposed approaches. Next, the reachability set is calculated using the convolution method by taking 100,000 MC points. These results are shown in the first column of Fig. 5 with time-varying from $t_1 = 1s$ to $t_7 = 7s$. In Fig. 5 the convolution contours are superimposed with the MC scatter points (shown in cyan colour). It can be observed that the convolution contours are able to capture the shape of the reachability set in a precise manner, by looking carefully at the figures. Further, the PME approach is employed using 10,000 MC points with the 2nd, 3rd and 4th order moment constraints. The variation of 3rd and 4th order constraints can be seen in the second and third column of Fig. 5 from time $t_1 = 1s$ to $t_7 = 7s$. The 2nd order approximation gives the ellipsoidal contours as shown in the first column of Fig. 6. Notice here that the contour levels are plotted at a similar level for all the three-moment constraint orders. It can be observed that with the inclusion of 3rd and 4th order in the approximation, the contours started to take the shape of the heuristic reachability set. Finally, the CUT method is utilized for computing the reachability set at these time instances. Notably, this method only used 21 CUT points for both 2D state and 2D control input. Since second-order moment constraint is only accounted, the $1 - \sigma$, $2 - \sigma$, $3 - \sigma$, $4 - \sigma$ and $5 - \sigma$ bounds come out to be of ellipsoidal shape and can be seen in the 2nd column of Fig. 6.

C. Dubin's Model

In this section, the above mentioned numerical techniques are applied to a Dubin's car model [45], which is a simple non-holonomic model for ground vehicle motion planning. Mathematically Dubin's model is:

$$\begin{aligned}\dot{x} &= v \cos \theta \\ \dot{y} &= v \sin \theta \\ \dot{\theta} &= \omega\end{aligned}\tag{37}$$

where x and y represent the position of the vehicle and θ is the heading angle. v is the forward velocity and ω is the angular velocity. The continuous time Dubin's model of Eq. (37) can be discretized by approximating time derivatives with a finite difference, as shown by Eq. (38).

$$\begin{aligned}x_{k+1} &= x_k + v \cos \theta_k \Delta t \\ y_{k+1} &= y_k + v \sin \theta_k \Delta t \\ \theta_{k+1} &= \theta_k + \omega \Delta t\end{aligned}\tag{38}$$

where Δt is the time step size between the two consecutive states. For calculating the reachability set, the control inputs v and ω are assumed to be uniformly distributed random variables within prescribed bounds given in Eq. (39).

$$10m/s \leq v \leq 20m/s, \quad -1deg/s \leq \omega \leq 1deg/s\tag{39}$$

To generate the ground truth, the reachability set is first computed through the Monte Carlo (brute force) sampling by taking all possible combinations of \mathbf{x}_k and \mathbf{u}_k at each time step. 100,000 MC samples for both the control input and initial state are taken with the time step size, Δt chosen as 0.5s. The evolution of reachability set at time $t_2 = 1s$, $t_3 = 1.5s$, $t_4 = 2s$ and $t_5 = 2.5s$ is shown in Fig. 7. Notice that x values are increasing in the positive direction due to $\cos\theta$ term, while the values in y are increasing symmetrically in both directions due to $\sin\theta$ term with an increase in time.

Furthermore, the reachability sets are generated through the application of PME using 100,000 MC points as shown in Fig. 8. The PME approximation of reachability set are superimposed with MC points (shown in cyan colour dots) by considering second, third, and fourth order statistical moments as constraints in PME formulation of Eq. (11)-Eq. (12). As expected the second order moment constraints results in an ellipsoidal approximation of the reachability set as can be seen in Figure 8(a) while the reachability set approximation improves with the inclusion of higher order moment constraints in PME formulations as illustrated in Figure 8(b) and Figure 8(c).

The comparison of each approach at time instances t_3 , t_4 and t_5 is shown in Fig. 9. The reachability sets generated using the convolution method is shown in Fig. 9(a), Fig. 9(d) and Fig. 9(g). This method utilizes 100,000 random samples of \mathbf{u}_k at each time and then convolved with the histogram of the previous time step to get the histogram at the current time step. Comparing these results with the MC plots, it can be seen that the convolution pretty accurately captures the whole region of the reachability set. For instance, at time t_3 shown in Fig. 9(a), the shape of the contours generated through the convolution is able to capture the shape of the whole domain of the MC points shown in cyan

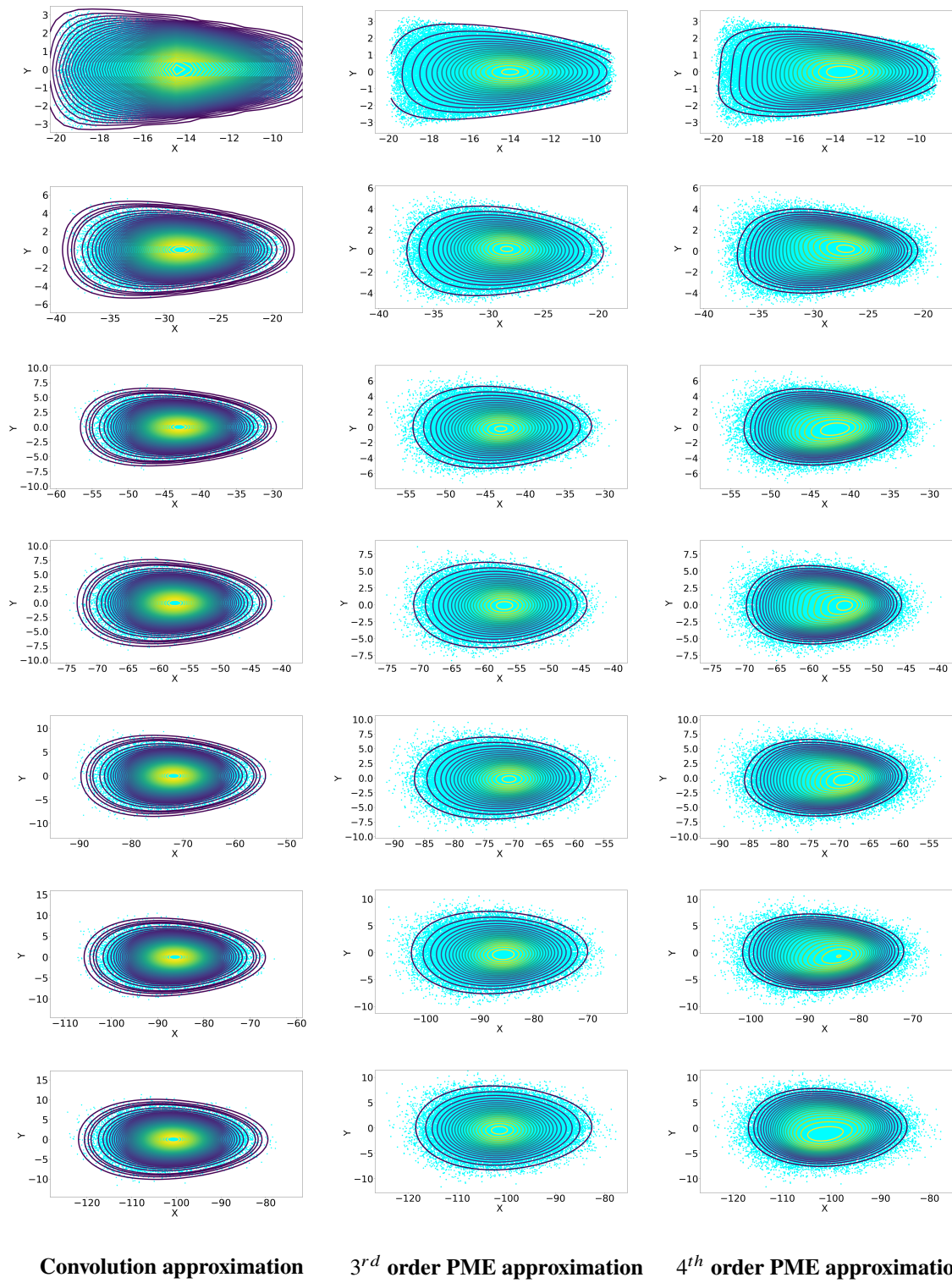
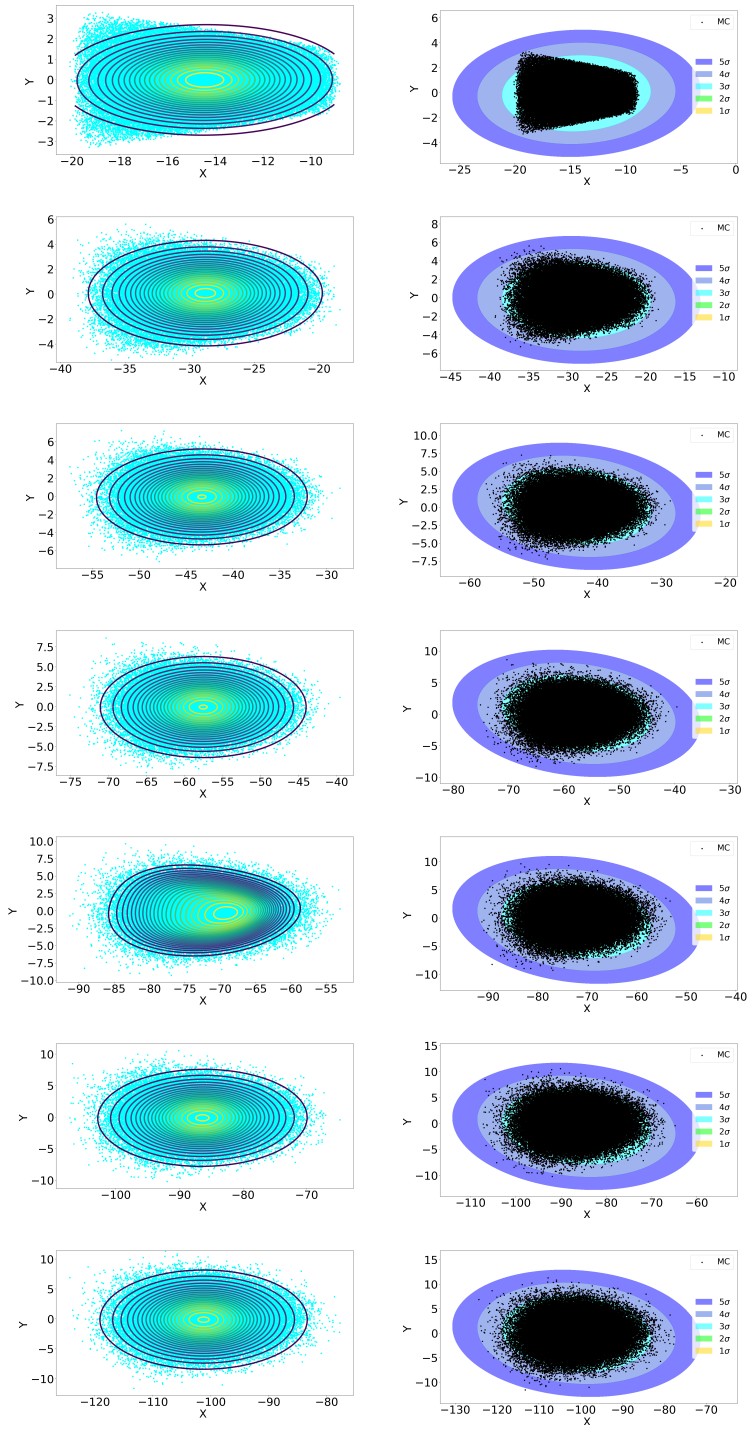


Fig. 5 Reachability Set of an Airplane computed using Convolution and PME



2nd order PME approximation 2nd order CUT approximation

Fig. 6 Reachability Set an Airplane computed through 2nd order PME and CUT method

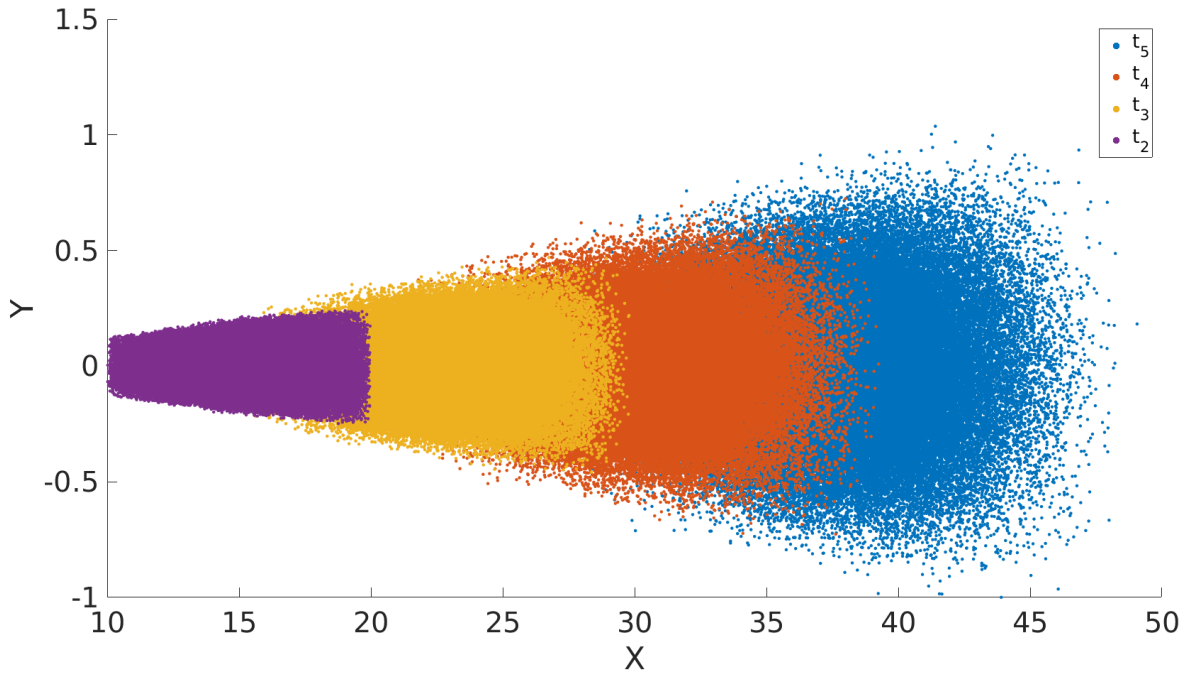
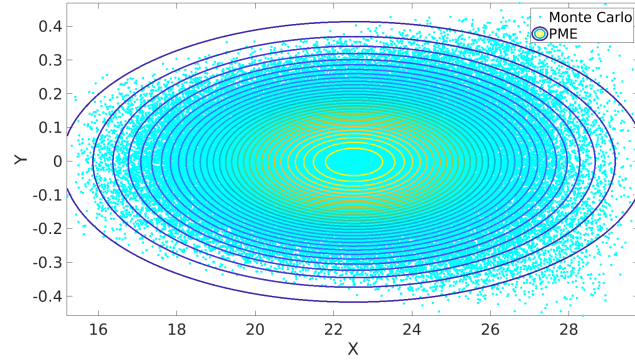
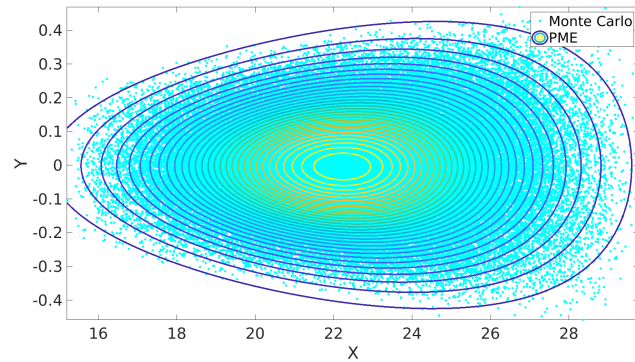


Fig. 7 Evolution of Reachability Set for Dubin's Model through MC

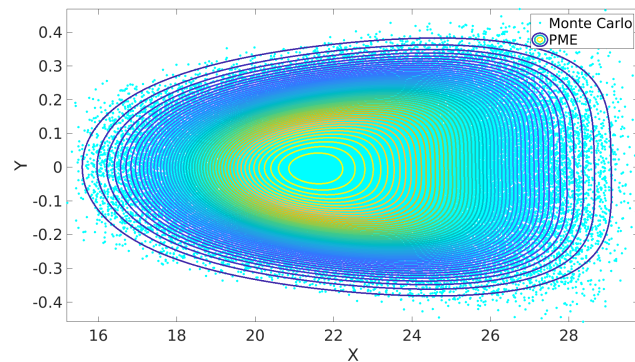
colour dots. For comparison, the 4th order PME reachability set is shown in Fig. 9(b), Fig. 9(e) and Fig. 9(h), which again captures the reachability in perfect, well shape and an accurate manner. Finally, the reachability envelope using the statistical moments is shown in Fig. 9(c), Fig. 9(f) and Fig. 9(i) where the uniform CUT8 samples for control and gaussian CUT8 samples for state are used (which results in only 21 points in 2D and 59 points in 3D). The $1 - \sigma$, $2 - \sigma$, $3 - \sigma$, $4 - \sigma$ and $5 - \sigma$ bounds can be seen in different colour shades along with MC samples, which are represented by black dots. This time, even though MC samples lie inside the 5-sigma bounds, the ellipsoidal contours do not match the shape of the MC envelope. This is due to the fact that the nature of the probability density function for the state at each time step is approximated to be Gaussian. In this case, only the first two statistical moments are used (the mean and covariance) to reconstruct the density function, hence the ellipsoidal shape.



(a) Moment up to 2^{nd} order



(b) Moment up to 3^{rd} order



(c) Moment up to 4^{th} order

Fig. 8 Reachability of Dubin's Model at t_3 computed through the application of PME

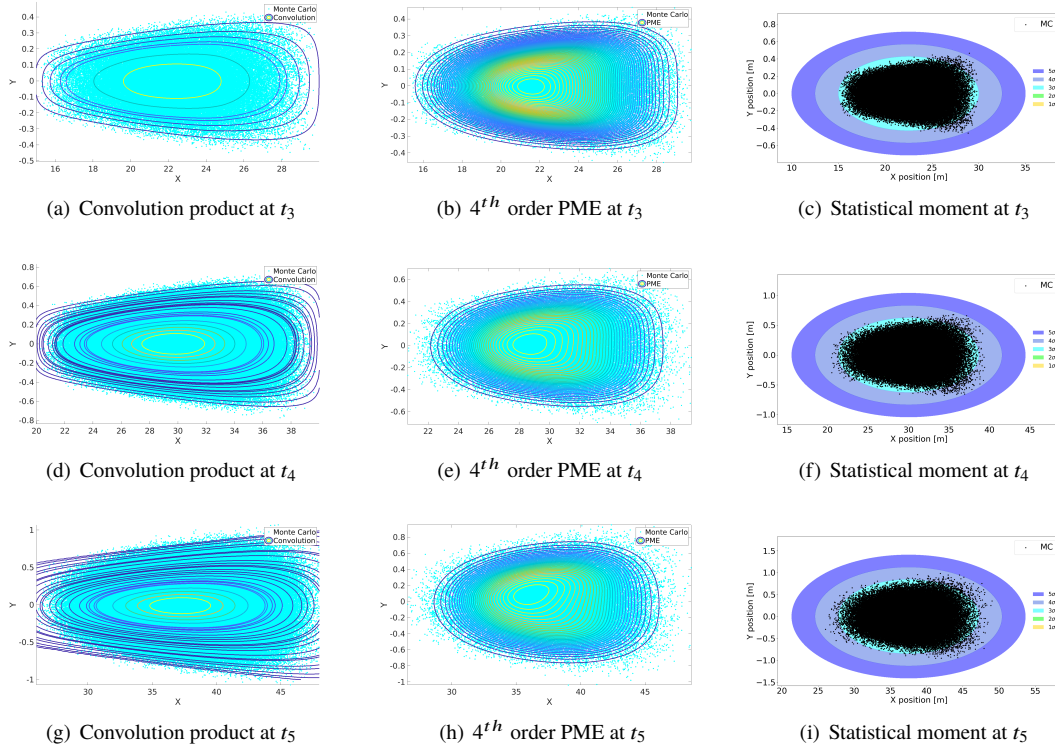


Fig. 9 Comparison of Different Approaches in Approximating Reachability Set for Dubin's Model

V. Conclusion

Computationally attractive approaches for evaluating the reachability of a nonlinear system are developed. The probabilistic approach presented in the paper provides a means of representing the reachability level sets as the state probability density function maps obtained by modeling the inputs as random vectors. By convolving the histograms of state and control at a previous time step, the convolution method computes the information of state at the current time step. By exploiting the intricate relationships of the moment generating functions of multivariate random variables to the probability density function, and building upon the principle of maximum entropy, the method demonstrates that the reachability set computation becomes tremendously simplified. Further, Conjugate Unscented Transformation (CUT) is used to compute multi-dimensional expectation integrals required to calculate desired order moments associated with state density function at each time. This approach exploits the independence of state variable and control input variable to curtail the conventional combinatorial growth of samples associated with the computation of reachability sets. Using the representative examples show the utility of the proposed approach in efficient realization of manifolds for constrained mechanical systems. The future work will focus on the incorporation of higher order moments through the CUT method.

References

- [1] Althoff, M., and Dolan, J. M., "Online verification of automated road vehicles using reachability analysis," *IEEE Transactions on Robotics*, Vol. 30, No. 4, 2014, pp. 903–918.
- [2] Henzinger, T. A., Ho, P. H., and Toi, H. W., *TACAS 95: Tools and algorithms for the construction and analysis of systems, Lecture Notes in Computer Science*, Springer, 1995, Vol. 1019, Chap. A user guide to HYTECH, pp. 41–71.
- [3] Botchkarev, O., and Tripakis, S., *Hybrid systems: Computation and control, Lecture Notes in Computer Science*, Springer, 2000, Vol. 1790, Chap. Verification of hybrid systems with linear differential inclusions using ellipsoidal approximations, pp. 73–88.
- [4] Chutinam, A., and Krogh, B., *Hybrid systems: Computation and control, Lecture Notes in Computer Science*, Springer, 1999, Vol. 1569, Chaps. Verification of polyhedral-invariant hybrid automata using polygonal flow pipe approximations, pp. 76–90.

- [5] Greenstreet, M., and Mitchell, I., *Hybrid systems: Computation and control, Lecture Notes in Computer Science*, Springer, 1998, Vol. 1386, Chap. Integrating projections, pp. 159–17174.
- [6] Kurzhanski, A., and Varaiya, P., *Hybrid systems: Computation and control, Lecture Notes in Computer Science*, Springer, 2000, Vol. 1790, Chap. Ellipsoidal techniques for reachability analysis, pp. 202–214.
- [7] Mitchell, I., and Tomlin, C., *Hybrid systems: Computation and control, Lecture Notes in Computer Science*, Springer, 2000, Vol. 1790, Chap. Level set methods for computation in hybrid systems, pp. 310–17323.
- [8] Jang, J. S., and Tomlin, C., “Control strategies in multi-player pursuit and evasion game,” *AIAA Guidance, Navigation, and Control Conference and Exhibit*, 2005, p. 6239.
- [9] Lygeros, J., “On reachability and minimum cost optimal control,” *Automatica*, Vol. 40, No. 6, 2004, pp. 917–927.
- [10] Löfberg, J., “YALMIP : A Toolbox for Modeling and Optimization in MATLAB,” *In Proceedings of the CACSD Conference*, Taipei, Taiwan, 2004.
- [11] Löfberg, J., “Pre- and post-processing sum-of-squares programs in practice,” *IEEE Transactions on Automatic Control*, Vol. 54, No. 5, 2009, pp. 1007–1011.
- [12] Mitchell, I. M., and Templeton, J. A., *Lecture Notes in Computer Science (LNCS) 3414: Hybrid Systems Computation and Control*, Springer-Verlag, 2005, Chaps. A Toolbox of Hamilton-Jacobi Solvers for Analysis of Nondeterministic Continuous and Hybrid Systems, pp. 480–494.
- [13] Lygeros, J., “Minimum Cost Optimal Control: An Application to Flight Level Tracking,” *Mediterranean on Control and Automation*, Rhodes, Greece., 2003.
- [14] Kitsios, I., and Lygeros, J., “Launch-pad Abort Flight Envelope Computation for a Personnel Launch Vehicle Using Reachability,” *AIAA Guidance, Navigation and Control Conference and Exhibit*, San Francisco, California, USA, 2005.
- [15] Kitsios, I., and Lygeros, J., “Aerodynamic Envelope Computation for Safe Landing of the HL-20 Personnel Launch Vehicle using Hybrid Control,” *Mediterranean on Control and Automation*, Nicosia, Cyprus., 2005.
- [16] Kurzhanskiy, A. A., and Varaiya, P., “Ellipsoidal toolbox (ET),” *Proceedings of the 45th IEEE Conference on Decision and Control*, IEEE, 2006, pp. 1498–1503.
- [17] Althoff, M., and Grebenyuk, D., “Implementation of Interval Arithmetic in {CORA} 2016,” *Proc. of the 3rd International Workshop on Applied Verification for Continuous and Hybrid Systems*, 2016.
- [18] Annichini, A., Bouajjani, A., and Sighireanu, M., “TRex: A tool for reachability analysis of complex systems,” *International Conference on Computer Aided Verification*, Springer, 2001, pp. 368–372.
- [19] Henzinger, T. A., Ho, P.-H., and Wong-Toi, H., “HyTech: A model checker for hybrid systems,” *International Conference on Computer Aided Verification*, Springer, 1997, pp. 460–463.
- [20] Majumdar, A., Vasudevan, R., Tobenkin, M. M., and Tedrake, R., “Convex optimization of nonlinear feedback controllers via occupation measures,” *The International Journal of Robotics Research*, 2014.
- [21] Tedrake, R., Manchester, I. R., Tobenkin, M. M., and Roberts, J. W., “LQR-Trees: Feedback motion planning via sums of squares verification,” *International Journal of Robotics Research*, Vol. 29, 2010, pp. 1038–1052.
- [22] Holzinger, M. J., and Scheeres, D. J., “Reachability results for nonlinear systems with ellipsoidal initial sets,” *IEEE transactions on aerospace and electronic systems*, Vol. 48, No. 2, 2012, pp. 1583–1600.
- [23] Allen, R. E., Clark, A. A., Starek, J. A., and Pavone, M., “A machine learning approach for real-time reachability analysis,” *Intelligent Robots and Systems (IROS 2014), 2014 IEEE/RSJ International Conference on*, IEEE, 2014, pp. 2202–2208.
- [24] Komendera, E., Bradley, E., and Scheeres, D., “Efficiently locating impact and escape scenarios in spacecraft reachability sets,” *AIAA/AAS Astrodynamics Specialist Conference*, 2012, p. 4810.
- [25] Jazwinski, A. H., *Stochastic Processes and Filtering Theory*, Academic Press Inc., New York, 1970.
- [26] Oppenheim, A. V., and Schaffer, R. W., *Discrete-time signal processing*, Pearson Education, 2014.
- [27] Cover, T. M., and Thomas, J. A., *Elements of Information Theory (Wiley Series in Telecommunications and Signal Processing)*, Wiley-Interscience, 2006.

- [28] Jaynes, E. T., "Prior Probabilities," *IEEE Transactions on Systems and Cybernetics*, Vol. 4, No. 3, 1968, pp. 227–241, DOI: 10.1109/TSSC.1968.300117.
- [29] Abramov, R. V., "The multidimensional moment-constrained maximum entropy problem: A BFGS algorithm with constraint scaling," *J. Comput. Phys.*, Vol. 228, No. 1, 2009, pp. 96–108.
- [30] Wu, Z., Phillips, J., George N., Tapia, R., and Zhang, Y., "A Fast Newton Algorithm for Entropy Maximization in Phase Determination," *SIAM Review*, Vol. 43, No. 4, 2001, pp. 623–642, DOI: 10.1137/S0036144500371737.
- [31] Abramov, R. V., "An improved algorithm for the multidimensional moment-constrained maximum entropy problem," *Journal of Computational Physics*, Vol. 226, No. 1, 2007, pp. 621–644, DOI: 10.1016/j.jcp.2007.04.026.
- [32] Fletcher, R., *Practical methods of optimization*, John Wiley & Sons, 2013.
- [33] Gerstner, T., and Griebel, M., "Numerical integration using sparse grids," *Numerical Algorithms*, Vol. 18, 1998, pp. 209–232. URL <http://dx.doi.org/10.1023/A:1019129717644>, 10.1023/A:1019129717644.
- [34] Stroud, A. H., and Secrest, D., *Gaussian Quadrature Formulas*, Englewood Cliffs, NJ: Prentice Hall, 1966.
- [35] Adurthi, N., Singla, P., and Singh, T., "The Conjugate Unscented Transform-An Approach to Evaluate Multi-Dimensional Expectation Integrals," Proceedings of the American Control Conference, 2012.
- [36] Adurthi, N., Singla, P., and Singh, T., "Conjugate Unscented Transformation: Applications to Estimation and Control," *Journal of Dynamic Systems, Measurement, and Control*, Vol. 140, No. 3, 2018, p. 030907.
- [37] Adurthi, N., "The Conjugate Unscented Transform - A Method to Evaluate Multidimensional Expectation Integrals," Master's thesis, University at Buffalo, 2013.
- [38] Adurthi, N., Singla, P., and Singh, T., "Conjugate Unscented Transform Rules for Uniform Probability density functions," Proceedings of the American Control Conference, 2013.
- [39] Adurthi, N., Singla, P., and Singh, T., "Conjugate Unscented Transform and its Application to Filtering and Stochastic Integral Calculation," AIAA Guidance, Navigation, and Control Conference, 2012.
- [40] Bursik, M., Jones, M., Carn, S., Dean, K., Patra, A., Pavolonis, M., Pitman, E. B., Singh, T., Singla, P., Webley, P., Bjornsson, H., and Ripepe, M., "Estimation and propagation of volcanic source parameter uncertainty in an ash transport and dispersal model: Application to the Eyjafjallajokull plume of 14–16 April 2010," *Bulletin of Volcanology*, Vol. 74, No. 10, 2012, pp. 2321–2338.
- [41] Madankan, R., Pouget, S., Singla, P., Bursik, M., Dehn, J., Jones, M., Patra, A., Pavolonis, M., Pitman, E. B., Singh, T., and Webley, P., "Computation of probabilistic hazard maps and source parameter estimation for volcanic ash transport and dispersion," *Journal of Computational Physics*, Vol. 271, 2014, pp. 39–59.
- [42] Adurthi, N., Singla, P., and Majji, M., "Conjugate Unscented Transform based approach for dynamic sensor tasking and Space Situational Awareness," *American Control Conference (ACC), 2015*, IEEE, 2015, pp. 5218–5223.
- [43] Adurthi, N., and Singla, P., "A Conjugate Unscented Transformation Based Approach for Accurate Conjunction Analysis," *AIAA Journal of Guidance, Control and Dynamics*, Vol. 38, No. 9, Sep. 2015, pp. 1642–1658.
- [44] Madankan, R., Singla, P., Singh, T., and Scott, P. D., "Polynomial Chaos based Bayesian Approach for State and Parameter Estimation," *AIAA Journal of Guidance, Navigation, and Control*, Vol. 36, No. 4, 2013, pp. 1058–1074.
- [45] Dubins, L. E., "On curves of minimal length with a constraint on average curvature, and with prescribed initial and terminal positions and tangents," *American Journal of mathematics*, Vol. 79, No. 3, 1957, pp. 497–516.
- [46] Majumdar, A., "Robust online motion planning with reachable sets," Ph.D. thesis, Massachusetts Institute of Technology, 2013.